Dielectric relaxation mechanisms in polyoxymethylene/polyurethane/layered silicates hybrid nanocomposites

G. N. Tomara[1], P. K. Karahaliou[1], G. C. Psarras[2], S. N. Georga[1], C. A. Krontiras[1], S. Siengchin[3], J. Karger-Kocsis[4,5]

[1] Department of Physics, University of Patras, Patras 26504, Greece

[2] Department of Materials Science, University of Patras, Patras 26504, Greece

[3] Department of Mechanical and Process Engineering, The Sirindhorn International Thai German Graduate School of Engineering (TGGS), King Mongkut's University of Technology North Bangkok, Bangkok 10800, Thailand

[4] Department of Polymer Engineering, Budapest University of Technology and Economics, H-1111 Budapest, Műegyetem rkp. 3, Hungary

[5] MTA-BME Research Group for Composite Science and Technology, Műegyetem rkp. 3, Budapest H-1111, Hungary

Abstract

Polyoxymethylene/Polyurethane/Layered Silicates (POM/PU/LS) ternary hybrid nanocomposites were prepared by two methods: (a) direct melt compounding (DM) and (b) melt compounding using a latex-mediated masterbatch (MB) technique. The morphology of the produced specimens and the quality of the dispersion of LS (synthetic sodium fluorohectorite) were examined via Scanning Electron Microscopy (SEM) and Transmission Electron Microscopy (TEM). Broadband dielectric spectroscopy (BDS) was employed in order to study the dielectric response of the two systems in a wide frequency and temperature range. Rich dielectric spectra are recorded, since dielectric relaxation mechanisms originate from POM matrix, PU latex as well as from interfacial phenomena between LS and the polymer matrix. Six different mechanisms were observed in the spectra of the examined

nanocomposites which are identified, in terms of decreasing temperature at constant frequency, as Maxwell-Wagner-Sillars (MWS) effect merged with contribution from the DC conductivity, α-mode of POM, α-mode of PU, γ- and δ-modes of POM and γ-mode of PU. The dynamics of the recorded processes as well as the effect of the preparation technique, on the way these processes are imprinted in the dielectric spectra of the examined systems, are considered and discussed.

1 Introduction

Polymer composites remain in the spotlight of the scientific research, since the beginning of the 1960s, as they are high performance materials with a wide variety of applications. Among their advantages is the combination of high mechanical strength, low weight, ease of processing and low cost. Nowadays polymer composites possess a leading position in various engineering applications [1]. In recent years, nanoinclusions offer new opportunities for designing advanced composite materials with novel properties. The superiority of nanocomposites, in comparison to their micro counterparts, is mainly attributed to the fact that nanoparticles exhibit high surface area-to-volume ratio compared to microparticles. As a result, nanocomposites exhibit significantly greater interfacial area for the same concentration of the filler, leading to the formation of an extended interaction zone where the polymer behaviour is altered from the bulk [2,3]. Moreover, nanocomposites have begun to gain ground in the field of dielectrics and electrical insulation, since it is assumed that fabrication of polymeric nanocomposites is one of the most effective approaches for the enhancement of the dielectric properties of polymers. By controlling the nanofiller dispersion and interfacial interactions in nanocomposites, dielectric properties can be tailored for specific applications [4]. Accordingly, the electrical response of polymer nanocomposites is of significant importance and requires thorough investigation.

Polyoxymethylene (POM) is a widely used engineering thermoplastic that is technologically important as it combines resistance against various solvents with enhanced thermomechanical properties [5-7]. Furthermore, it exhibits low water absorption and good electrical insulation properties, rendering it as a perfect candidate for electrical and electronic applications [8]. On the other hand, the high degree of crystallinity of POM accompanied by brittleness is a limiting factor for its applications [9,10]. Blending POM with thermoplastic polyurethane (PU) is often proposed as a reliable solution for POM toughening [11-13].

A variety of methods have been developed for the preparation of POM based nanocomposites, including in situ polymerization, melt blending, and solution/dispersion techniques, aiming to overcome serious challenges and achieving uniform dispersion of the nanofiller in the polymer matrix and obtaining good interfacial adhesion between the nanoparticles and the polymer [14].

Within the framework of the present work, we examine the influence of the preparation technique on the morphological characteristics and on the dielectric response of POM/PU/LS ternary systems prepared by two methods: (a) direct melt (DM) compounding and (b) latex-mediated masterbatch (MB) technique. For this reason, the morphology of the systems and the dispersion of the LS were tested via Scanning and Transmission Electron Microscopy (SEM, TEM). Additionally, for the examination of the dielectric response, Broadband Dielectric Spectroscopy (BDS) was employed in a wide temperature and frequency range.

The relaxation mechanisms of POM and POM based systems have been the subject of extended studies, via both mechanical and dielectric techniques, since 1960s [8, 15-31]. Recently, the study of the dielectric response of POM and POM based nanocomposites offered a full dielectric relaxation map for POM and successfully contributed to the elimination of previous ambiguities concerning the identification of certain relaxation mechanisms [32]. So far four relaxations are identified assigned as α, β, γ, and δ-modes in

terms of decreasing temperature at constant frequency. The slower α-mode is attributed to translational motions along the polymer chain which take place at the surface of the crystallites. β-mode is of cooperative character and associated with the glass to rubber transition. This mode, that is affected by changes in the crystallinity [16,28,33,34], is mostly marked dielectrically in copolymers and polymer blends where the crystallinity of POM is reduced compared to the pure POM [23,28,35]. It was also marked in POM/Alumina nanocomposites but was absent from the dielectric spectra of POM/LS and POM/PU/Alumina systems previously studied by our group [32,36]. Within several studies the faster relaxation modes are commonly imprinted in the dielectric or Dynamic Mechanical Analysis (DMA) results as one broad peak [8,17,23]. It is now clear that this peak results from the summation of two different mechanisms [23,32]: i.e. the faster one denoted as δ-mode and the other one, at lower frequencies, assigned as γ-mode. The latter (γ-mode) is connected with hydroxyl end groups and/or local twisting motions of the main chain that mainly take place in the disordered regions of the bulk polymer [17], thus related to the amorphous phase whereas δ-mode is attributed to defect dipoles in the crystalline phase of POM.

The incorporation of PU into the POM matrix is expected to contribute to the overall dielectric response of the composite system. Pure PU systems have been examined both mechanically [16] and dielectrically [37-39]. The results of these two methods are in good agreement, revealing three relaxation mechanisms for PU, namely α, β and γ modes recorded with increasing temperature at constant frequency. α-Mode dominates the dielectric spectra and is related to the glass to rubber transition of PU. The intermediate β-relaxation is comparatively weaker than the other two and involves absorbed water molecules attached by hydrogen bonds to the PU chains while, the faster relaxation observed, γ-mode, is associated with the motions of the methylene groups between amide groups in the polymer chain.

Furthermore, the nanoinclusions are expected to contribute to the dielectric response through the emergence of the Maxwell-Wagner-Sillars (MWS) effect that is attributed to the accumulation of free charges at the filler-matrix interface. In the case of POM that is a semicrystalline polymer, this effect is even more pronounced as charges can also accumulate at the interface of the amorphous and the crystalline regions of POM [32,36].

2 Experimental

2.2 Materials

Blends of granulated POM (Hostaform C 9021, Ticona GmbH, Frankfurt, Germany) and latex of thermoplastic PU with 50 wt % dry content (Acralen U 550 supplied by Polymer Latex Marl, Germany), were used as polymer matrix [36]. Water-swellable sodium fluorohectorite (layered silicate-LS, Somasif ME-100, Coop Chemicals,Tokyo, Japan) was used as nanofiller. LS is characterized by an interlayer distance of 0.92 nm and a cation exchange capacity of 100 mequiv/100 g. The nominal aspect ratio of layered silicate is close to 1000 (according to suppliers' information).

Ternary POM/PU/LS hybrid nanocomposites were prepared by two methods: (a) direct melt compounding (DM) and (b) melt compounding using a masterbatch containing both PU and LS (MB technique). The content of PU was kept constant at 10 wt% and the content of LS at

3 wt%. Melt mixing occurred in laboratory kneader (Type 50 of Brabender, Duisburg, Germany) at 190°C and rotor speed of 60 rpm. LS filler (DM technique) or LS-containing PU (MB technique) was introduced in the POM system following melt mastication of the latter for 2 min. The duration of the melt mixing for both DM and MB techniques was 6 min. Then, the compounds were compression moulded into 1 mm-thick sheets at 200°C using a hot press (EP-Stanzteil, Wallenhorst, Germany).

2.2 Characterization techniques

The morphology of the samples and the dispersion of layered silicates were inspected using Scanning Electron Microscopy (SEM; SupraTM 40VP SEM f Carl Zeiss GmbH, Oberkochen, Germany) and Transmission Electron Microscopy (TEM; Zeiss LEO 912 Omega apparatus), applying an acceleration voltage of 120 kV. Thin sections of 50 nm were cut at RT with a Diatome diamond knife (Hatfield, PA) using an Ultracut E microtome (Reichert and Jung, Vienna, Austria).

The ternary systems were electrically characterised by Broadband Dielectric Spectroscopy (BDS) in the frequency range of 0.1 Hz to 1 MHz using Alpha-N Frequency Response Analyser, supplied by Novocontrol Technologies (Hundsagen, Germany). Isothermal frequency scans were conducted in the temperature range from -110°C to 150°C in steps of 10°C. Temperature was controlled within ± 0.1°C by the Quattro system and the applied ac voltage was Vrms = 1.0 V. The BDS-1200 parallel-plate capacitor with two gold plated electrodes, also supplied by Novocontrol, was used as test cell. The cell was electrically shielded and the sample was kept within nitrogen gas atmosphere. WinDeta software was used for controlling of the system and data acquisition and WinFit software was employed for the analysis of the experimental data.

3 Results

3.1 Morphology-SEM-TEM

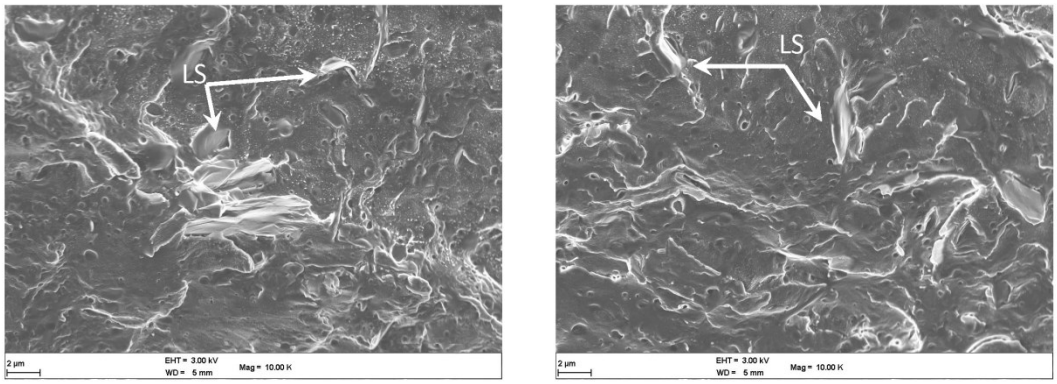

Fig.1. *SEM images of POM/PU/LS nanocomposites produced via DM compounding (a) and MB technique (b). Note: holes and spherical domains represent PU and arrows indicate for LS.*

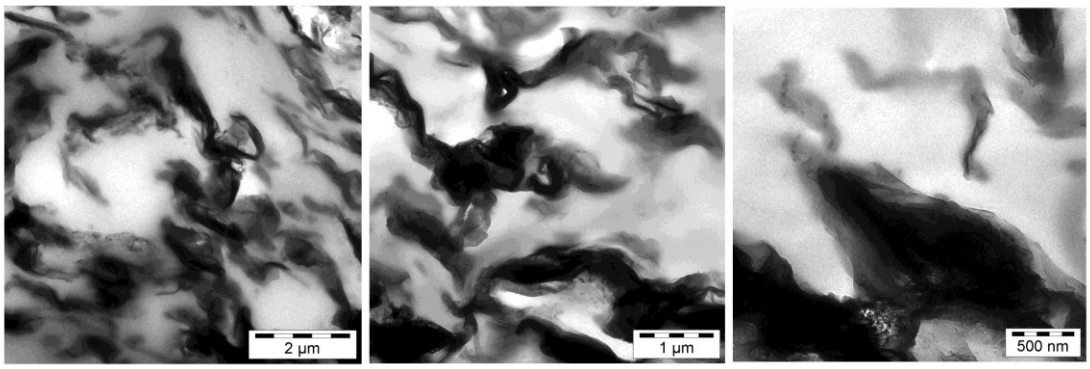

Fig.2. *TEM images of POM/PU/LS composites produced via the MB technique.*

In order to study the morphology of the specimens, SEM and TEM pictures were taken from the fracture surfaces and thin sections (ca.50 nm), respectively. The dispersion of layered silicates and PU in the POM/PU/LS composites produced by direct melt mixing (fig 1a) and melt compounding using masterbatch technique (fig 1b) are presented in figure 1. It is evident that PU rubber particles are well dispersed in the POM matrix irrespectively of the preparation technique. Moreover SEM images reveal that LS are mostly dispersed in the POM matrix and/or close to the POM/PU interface. Nevertheless, agglomerations of LS are present in the microscale in both systems, being more evident in the case of the DM produced nanocomposites. Thus, a better dispersion of the LS in the POM/PU/LS (MB) system is achieved. TEM images of MB produced specimens (fig 2) also show that the layered silicates are predominantly intercalated which means that layer silicate stacks composed of several platelets with strongly reduced apparent aspect ratio, compared to a fully exfoliated LS structure, are present.

3.2 Dielectrics

The frequency and temperature variation of the imaginary part of electric modulus (M") for the POM/PU/LS (DM) and POM/PU/LS (MB) specimens is presented in figures 3a and 3b, respectively. Feature dielectric spectra are recorded in both cases, since dielectric relaxation mechanisms originating from POM and PU matrices, the LS reinforcing phase as well as interfacial phenomena are expected to contribute to the overall response of the nanocomposites. In the dielectric spectra of the POM/PU/LS (DM) system (figure 3a) six distinct relaxation peaks are present. On the other hand in the case of the POM/PU/LS (MB) system (figure 3b), while a similar high temperature response (for temperatures above 0°C) is observed, at lower temperatures (from -100°C to -40°C) the spectrum is dominated by a unique broad relaxation peak. It is well known that ascribing relaxation peaks, in an isochronal or isothermal dielectric plot to particular types of molecular motions and more interestingly to specific relaxing polar entities, is a complicated procedure and becomes even more intricate for complex systems [7,17,18,36]. As a result, for the ternary systems of the current study, an initial identification of the relaxation mechanisms contributing to the recorded dielectric response is attempted taking into account the dielectric behaviour of similar binary or ternary systems previously studied by our group, such as POM and/or PU based nanocomposites [7,32,36]. The slower relaxation in the high temperature and low frequency area of both POM/PU/LS (DM) and POM/PU/LS (MB) spectra is attributed to interfacial polarisation phenomena (Maxwell-Wagner-Sillars (MWS) effect), as well as to the contribution of the DC conductivity, denoted as conductivity term (CT) (merged CT and MWS) [17]. MWS effect, which is common in all heterogeneous, as well as in semicrystalline systems, is related to the accumulation of charges at the interfaces (filler-matrix and crystalline-amorphous phase interfaces) of the composite where they form dipoles, which are able to follow the oscillation of the electric field at low frequencies and high temperatures [40,41]. At lower temperatures and at constant frequency, α-modes of POM and PU are detected in agreement with previously reported results in POM/PU/Alumina nanocomposites [36]. It is obvious, from the 3D plots of figure 3, that α-mode of POM and α-mode of PU form two distinct relaxation peaks at lower temperatures merging in one broad peak as the temperature increases. The overlapping of the two relaxations is more pronounced in the case of POM/PU/LS (MB) system. In the middle area of the dielectric spectra of figures 3a,b and at the low frequency region, a weak relaxation peak is recorded, assigned to β-mode of PU [36] and attributed to local motions of polar side groups of the PU polymer chain imposed by the electric field [36, 37]. The intensity of this mechanism is relatively weak and not well imprinted in the dielectric spectra. As a result this relaxation could not be studied in detail. Finally, at the low temperature regime two relaxation peaks are recorded in the case of POM/PU/LS (DM) system. A similar behaviour has been previously observed in POM/LS systems, where the two relaxations have been assigned as γ- and δ-modes of POM [32]. The same assignment is applicable in the present case of the systems under study. However, since PU is also included in the nanocomposites of the current work, one should not overcome the fact that γ-relaxation of PU has also been recorded in previous published reports in the same frequency and temperature range [7,36]. Taking this into account, it is suggested that γ-mode of PU is also incorporated/hindered within the recorded peaks. The situation becomes even more puzzling in the case of the

POM/PU/LS (MB) system, where only one broad peak is formed in the low temperature regime of the dielectric spectrum. This unique peak appears much more intense than the separate peaks of the former case and its shape becomes broader, suggesting that more than one relaxation mechanisms are expected to contribute to its formation.

Thus, it is evident from the complexity of the dielectric spectra recorded for the ternary systems under study that, a deconvolution of the dielectric peaks is necessary in order to analyse and comment on the relaxation dynamics as well as on the effect of the preparation procedure on the dielectric response of the nanocomposites. For that reason the dielectric response of the samples, together with the deconvolution procedure is presented, separately for the low (-100°C to -40°C) and high (0°C to 150°C) temperature regions in the following section.

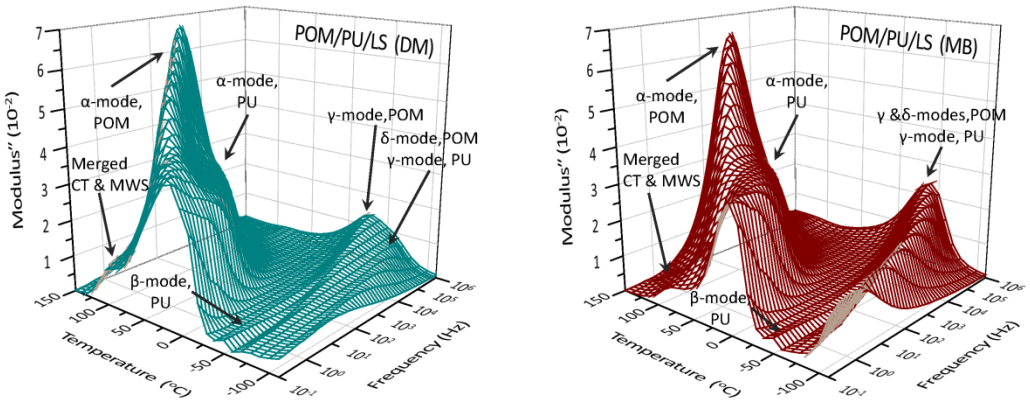

Fig.3. *Frequency and temperature variation of the imaginary part of electric modulus (M") for the POM/PU/LS nanocomposite produced via (a) DM compounding and (b) MB technique. In the plots MWS and CT stand for Maxwell-Wagner-Sillars effect and conductivity term respectively.*

4 Discussion

Figure 4 (a and b) represents the low temperature response, via the loss factor representation, of the two examined systems. The isothermal plots, at -90 °C, included in the inset of figure 4a correspond to pure PU and POM/LS systems, previously studied by our group, and are given here for reasons of comparison [32, 36]. In POM/PU/LS (DM) two relaxation peaks are clearly formed that, using the inset as a reference, are attributed to γ- and δ-mode of POM. However, the fact that at the same temperature and frequency region γ-mode of PU is also present suggests that the interplay of this mode cannot be neglected. In the case of POM/PU/LS (MB) system a unique peak is recorded in the low temperature region.

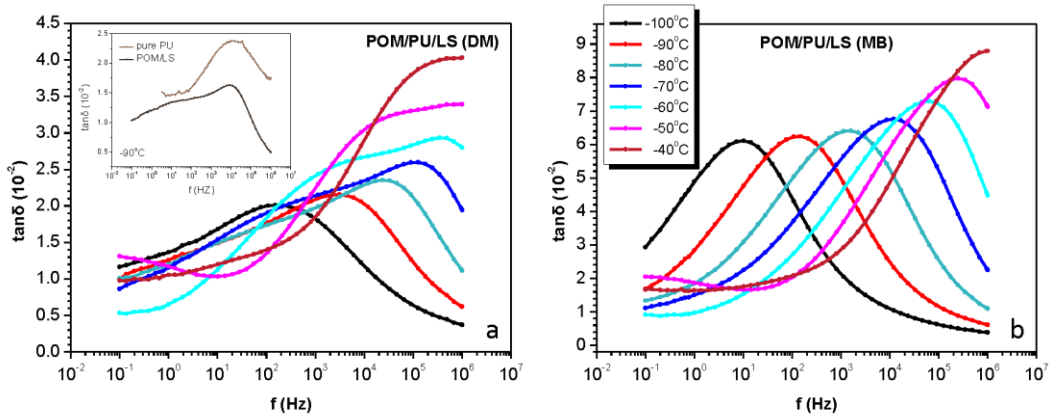

Fig.4. *Loss factor versus frequency for the (a) POM/PU/LS (DM) and (b) POM/PU/LS (MB) system in the low temperature region.*

A deconvolution of the relaxation peaks obtained in both POM/PU/LS (DM) and POM/PU/LS (MB) systems is attempted, assuming initially that all three mechanisms, i.e. γ- and δ-mode of POM and γ-mode of PU contribute to the obtained dielectric response. Through the deconvolution procedure the experimental data are fitted using equation (1):

$$\varepsilon(\omega) = \sum_{k} \Delta\varepsilon_k(\omega) + \varepsilon_\infty - i\left(\frac{\sigma_{DC}}{\omega\varepsilon_0}\right)^N \tag{1}$$

where, σ_{DC} and ε_∞ being the DC conductivity and the high frequency permittivity, respectively. N is a fitting parameter (usually taking values close to unity) which corresponds to the slope of the increase in ε" due to DC conductivity, occurring at low frequencies. Equation (1) represents the complex dielectric response as a sum over separate relaxation modes k, where each one can be characterized by a function $\Delta\varepsilon_k(\omega)$, which can be fitted to the following Havriliak–Negami function [42-46]:

$$\Delta\varepsilon_k(\omega) = \frac{\Delta\varepsilon_k}{(1 + (i\omega\tau_k)^{a_k})^{\beta_k}} \tag{2}$$

In equation (2), $\omega = 2\pi f$ and $\Delta\varepsilon_k = \varepsilon_r - \varepsilon_\infty$ is the difference between the relaxed and the unrelaxed values of the dielectric constant, also known as dielectric strength of the corresponding mode. The parameters α_k and β_k ($0 < \alpha, \beta < 1$) describe the symmetric and the asymmetric broadening of the equivalent relaxation time distribution function, respectively. τ is the Havriliak-Negami relaxation time and it is related to the loss peak relaxation time $\tau_{\max} = 1/2\pi f_{max}$ by equation (3):

$$\tau_{max} = \tau \left[\frac{\sin\left(\frac{\pi\alpha\beta}{2+2\beta}\right)}{\sin\left(\frac{\pi\alpha}{2+2\beta}\right)} \right]^{1/\alpha} \tag{3}$$

The fitting results for the two systems at -90°C are presented in figure 5 (a and b), where k in equation (1) equals to 3. Both dielectric spectra of figure 5 are satisfactorily reproduced by the summation of the three distinct relaxation mechanisms (γ-, δ- modes of POM and γ-mode of PU). However, the contribution of γ-mode of PU is significantly smaller than the one of γ- and δ-modes of POM, especially in the case of the POM/PU/LS (MB) system, where γ-mode of PU appears as a weak peak located at the left side of the frequency domain and shifts outside the measuring frequency window at higher temperatures (see for example -80°C in figure 6). The deconvolution procedure was applied to each separate temperature.

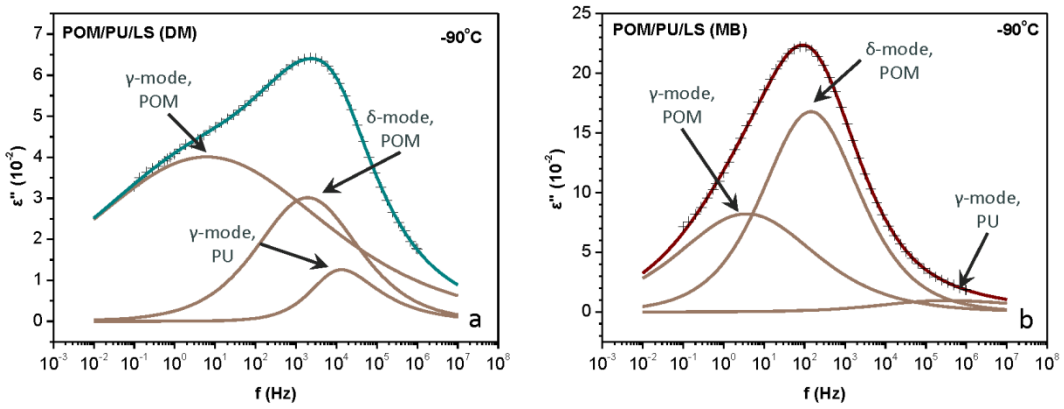

Fig.5. *Deconvolution of the dielectric loss spectra (ε") into the γ-mode and δ-mode of POM and γ-mode of PU in the frequency domain for (a) POM/PU/LS (DM) and (b) POM/PU/LS (MB) system, at -90˚C.*

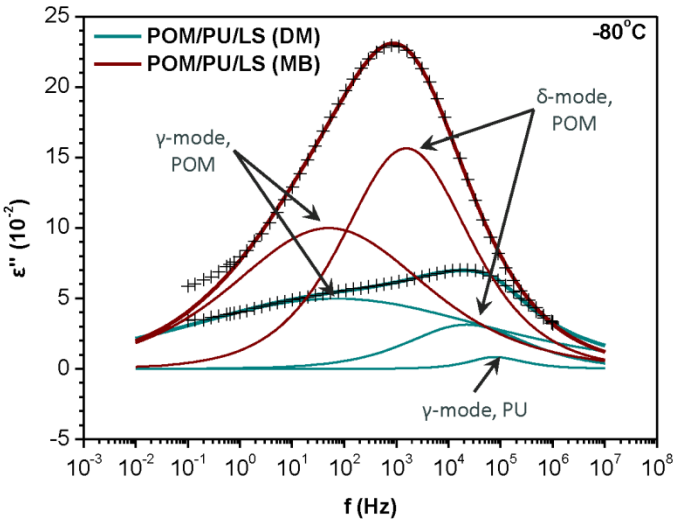

***Fig.6**. Comparative graph of the fitted results of dielectric loss ε" versus frequency for the POM/PU/LS (DM) and POM/PU/LS (MB) systems, at -80°C.*

Figure 6 presents the comparison of the fitted results and the overall curve at -80°C for the two preparation methods. It can be observed that, the peaks that correspond to γ-mode of POM lie close in frequencies and their magnitude is not altered significantly. In particular, the dielectric relaxation strength (Δε) calculated from the fitting procedure at -80°C equals 0.6 for POM/PU/LS (DM) and 0.7 for POM/PU/LS (MB). It is therefore concluded that γ-mode of POM is not significantly affected by the preparation method. This is in agreement with previous results in POM/PU/boehmite alumina systems, where γ-mode appears also unaffected by the preparation technique or by the inclusion of PU and/or Alumina nanofiller [36]. Since γ-relaxation is associated with motions taking place in the amorphous phase of the polymer it is not expected to be affected by the preparation technique or the addition of the nanofiller. In fact, the strength and the relaxation rate of this process is reported to be relatively insensitive even to changes in the molecular environment [17] and appears to be affected only by plasticization effects caused by moisture absorption [29] which is not the case in our systems.

On the other hand, δ-mode that is attributed to defect dipoles in the crystalline phase of POM is greatly influenced by the preparation technique. In particular, the dielectric relaxation strength (Δε) calculated from the fitting procedure at -80°C equals 0.1 for POM/PU/LS (DM) and increases to 0.8 for POM/PU/LS (MB) while the loss peak maximum is located at lower frequency in the case of the latter system.

The substantial increase of the dielectric strength suggests an increase of the dislocations or defects in the crystallites where δ-relaxation is taking place, attributed for instance to the better dispersion of LS in the POM/PU/LS (MB) system as indicated by the SEM results. In other words this substantial enhancement of the dielectric strength suggests an increase of the number of the defect dipoles and/or an increase of the dipolar moments [46], explaining the shift of the relaxation frequency to lower values.

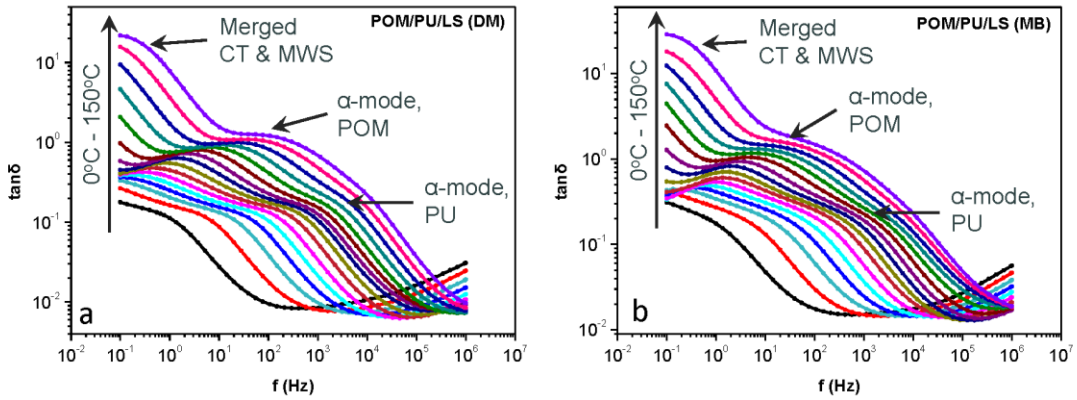

Fig.7. *Loss factor versus frequency for the (a) POM/PU/LS (DM) and (b) the POM/PU/LS (MB) systems in the high temperature region. In the plots MWS and CT stand for Maxwell-Wagner-Sillars effect and conductivity term respectively.*

The high temperature response (0°C to 150°C) of the studied systems is presented in figure 7, through the loss tangent representation. In this temperature region α-modes of POM and PU are expected to evolve. In fact, in the isothermal plots of figure 7 these two mechanisms appear to overlap and fitting procedure by the Havriliak-Negami equation was again applied to separate and study the individual contributions. At the low frequency edge of the spectra and at temperatures higher than 100°C an increase of the loss tangent is observed that eventually results to a peak formation at 150°C. This mechanism, which is also detected as a hump at the low frequency and high temperature edge of the three dimensional plots of figure 3, is attributed to interfacial polarisation phenomena (MWS) and/or to the contribution of the DC conductivity.

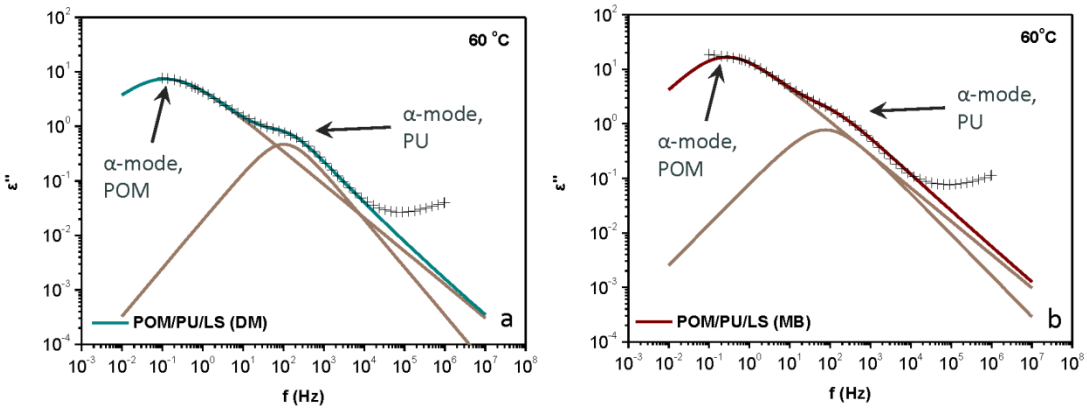

Fig.8. *Deconvolution of the dielectric loss ε" versus frequency into the α-modes of PU and POM in the frequency domain for the (a) POM/PU/LS (DM) and (b) POM/PU/LS (MB) systems at 60°C.*

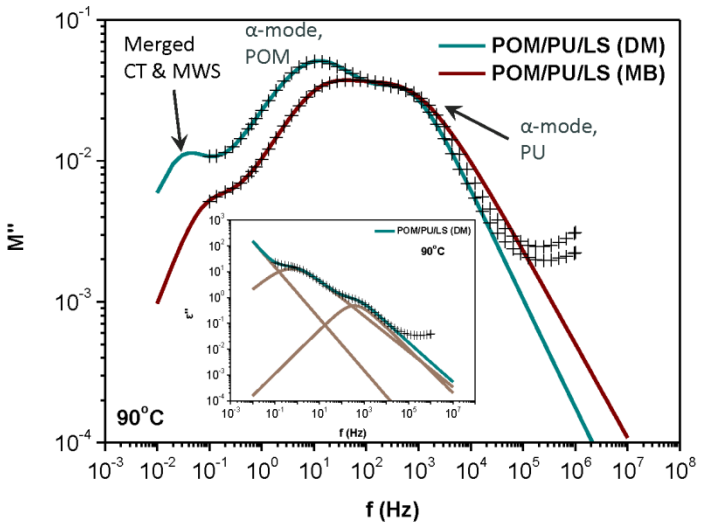

Fig.9. *Comparative graph of the fitting results in dielectric modulus M" representation for the POM/PU/LS (DM) and POM/PU/LS (MB) systems at 90°C. Inset: Deconvolution of the dielectric loss ε" versus frequency into the α-modes of PU and POM and the conductivity term (CT) in the frequency domain for the POM/PU/LS (DM) system at the same temperature. In the plots MWS and CT stand for Maxwell-Wagner-Sillars effect and conductivity term respectively.*

The deconvolution results for the POM/PU/LS (DM) and POM/PU/LS (MB) systems at 60°C are presented in figures 8(a) and 8(b), respectively and a comparative graph at 90°C is given in figure 9 indicatively. The same deconvolution procedure was applied in each separate temperature. While two Havriliak-Negami terms, corresponding to α-modes of POM and PU, were adequate for the fitting at 60°C, at higher temperatures an extra term has been used in order to account for the contribution of the DC conductivity. The fitting was performed simultaneously to the real and imaginary parts of dielectric permittivity (see for example figure 8 and inset of figure 9) and the fitting parameters were subsequently used for the theoretical reproduction of all the other representations of the dielectric data (see for example the fitting of M" data by the theoretically reproduced curve in figure 9). The above procedure was successfully followed for temperatures ranging from 20°C to 100°C and it is evident that the obtained theoretical curves satisfactorily fit the experimental data. Nevertheless, for temperatures above 100°C the fitting procedure could not be performed unambiguously and for that reason the obtained fitting results are not presented here and are not taken into account for the study of the relaxation dynamics. In particular, in these temperatures (>100°C) the merging of the two relaxation peaks (α-mode of POM and α-mode of PU) and more importantly the emergence of the DC conductivity which suppresses the formation of the relaxation peaks raises the degree of uncertainty and renders the fitting procedure non trivial.

It is clear from figures 8 and 9 that neither the loss peak position nor the shape of α-peak of PU are affected by the preparation procedure. Since this mode (α-mode) is connected to the glass to rubber transition of PU, one can claim that the T_g of PU remains practically constant irrespectively of the blending method. On the other hand, a shift of the loss peak maximum of α-mode of POM to higher frequencies is obtained for the POM/PU/LS (MB) system in comparison to its DM produced counterpart. Since this mode is attributed to main chain motions at the surface of the crystallites, frequency shifts of α-relaxation of POM are usually

attributed to changes in the degree of crystallinity or in the size of the crystallites [16, 19, 47]. Nevertheless, the experimental techniques employed in the present work (SEM and BDS) are not suitable to distinguish changes in the crystallinity or the crystallite size and more importantly, the preparation procedures are not expected to alter the crystallinity of the produced nanocomposites. Thus, the origin of this α-mode shift is not clear. One could only propose a possible loosening of the polymer chains close to the crystallites as the mechanism towards the observed shift, a fact which, however, needs further investigation.

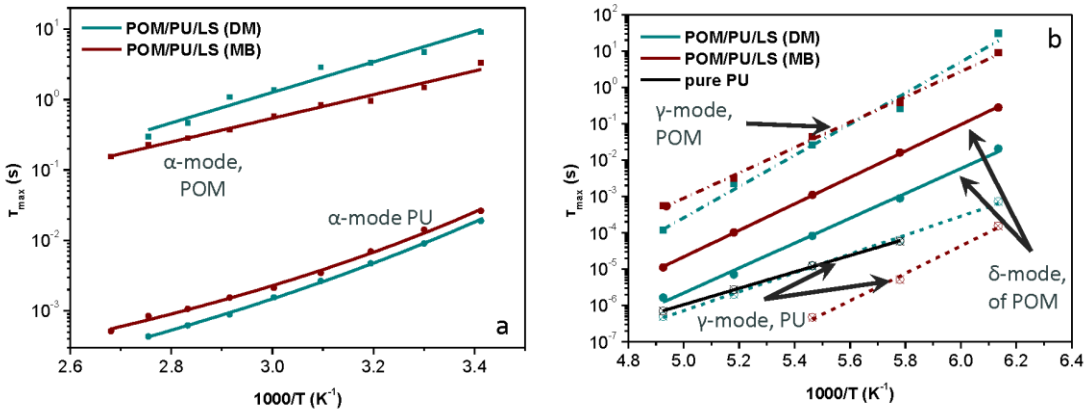

***Fig.10**. Relaxation time versus inverse temperature for the (a) low and (b) high temperature modes of POM/PU/LS (DM) and POM/PU/LS (MB) systems.*

The relaxation dynamics of all detected processes for POM/PU/LS (DM) and POM/PU/LS (MB) systems are depicted in figure 10. In this figure the Arrhenius plot of γ-mode of pure PU is also included for reasons of comparison. All relaxations of POM (δ-mode, γ-mode and α-mode) follow an Arrhenius type temperature dependence described by equation (4):

$$\tau_{max} = \tau_o e^{\frac{E_\alpha}{k_B T}} \quad (4)$$

where τ_o is a preexponential factor, E_α is the activation energy and k_B is the Boltzmann constant. τ_{max}, calculated from the fitting procedure via the Havriliak-Negami equation, were afterwards theoretically fitted to equation (4). The activation energies E_α of all four relaxation mechanisms exhibiting Arrhenius behaviour, are listed in Table 1. On the other hand, α-mode of PU exhibits a Vogel-Tamann-Fulcher (VTF) temperature dependence described by equation (5):

$$\tau_{max} = \tau_o e^{\frac{B}{T - T_o}} \quad (5)$$

where τ_o is a preexponential factor, B is a constant (measure of the activation energy) and T_o is the Vogel temperature or ideal T_g [36,37]. The VTF parameters, evaluated by the theoretical simulation of the results for the α-relaxation of PU to equation (5), are also listed in Table 1.

***Table 1**. Activation energies of the low temperature relaxations, as calculated from the fitting results, for all compared systems.*

sample	α mode POM	α mode PU		γ mode POM	δ mode POM	γ mode PU
	E_A (eV)	B (K)	T_o (K)	E_A (eV)	E_A (eV)	E_A (eV)
POM/PU/LS (DM)	0.43	1395	165	0.85	0.68	0.52
POM/PU/LS (MB)	0.33	994	185	0.69	0.72	0.75
pure PU						0.45

It is evident from figure 10 and table 1 that the activation energy of γ-mode of POM equals to 0.85eV in the case of POM/PU/LS (DM) system, in good agreement with previously published results for POM/LS systems [32]. The activation energy decreases slightly in the case of POM/PU/LS (MB) taking a value of 0.69eV, which is quite close to the value reported previously for POM/PU/ boehmite alumina systems [36]. It is also clear the frequency shift of δ-mode by almost one order of magnitude, which however does not affect its dynamics. The activation energy of δ-mode takes a mean value of 0.70eV which is increased in comparison to the activation energy of the same mechanism in the case of POM/LS systems (0.54eV) [32], implying that δ-mode is impeded by the blending of POM with PU. Finally, γ-mode of PU is tracked, in the case of POM/PU/LS (DM) system, at the same frequency region and possesses almost the same dynamics as in pure PU. The activation energy of 0.75eV obtained for the γ-mode of PU in the case of MB produced systems, appears significantly increased compared to the value of 0.52eV obtained for the DM systems. Note however, that the fact that this mode is detectable only in three temperatures in the MB system, the corresponding Arrhenius plot included in figure 10 is only indicative and the value of the calculated activation energy is probably not reliable. The evaluated activation energies for α-mode of POM in both DM and MB systems appear significantly smaller compared to typical values of the activation energy reported previously for pure POM being close to 1eV [16,32]. This reduction of the activation energy seems however to be in agreement with a similar reduction reported in other POM/PU based composites with boehmite alumina nanofillers [36]. Finally the VFT parameters evaluated for both systems are close to each other and in good agreement with the corresponding parameters for POM/PU and POM/PU/ boehmite systems [36].

5 Conclusions

A comparative study of the structural characteristics and the dielectric response of POM/PU/LS ternary hybrid nanocomposites produced by direct melt (DM) compounding and latex-mediated masterbatch (MB) techniques, is presented. The morphological examination conducted via SEM and TEM reveals that rubber particles are well dispersed in the POM matrix whereas, LS are mostly dispersed in the POM matrix and/or at the POM/PU interface, with better dispersion achieved in the case of MB produced nanocomposites.

The dielectric spectra of both systems are rich in relaxation modes since, mechanisms originating from the POM matrix, the PU latex and the presence of LS, contribute to the composites' dielectric response. A deconvolution procedure was followed for each measured temperature in order to identify the individual dielectric modes and study their dynamics. Specifically, six relaxation mechanisms are recorded which are, in terms of decreasing temperature Maxwell-Wagner-Sillars (MWS) effect merged with DC conductivity, α-mode of POM, α-mode of PU, γ- and δ-modes of POM and γ-mode of PU. The dynamics of all detected modes were analysed and the activation energies or VTF parameters were calculated. The analysis of the dielectric data reveals the following:

(i) The dielectric relaxations (α-and γ-) of PU remain unaffected by the incorporation of PU into POM matrix, irrespectively of the preparation technique.

(ii) γ-mode of POM, being attributed to the amorphous phase, remains essentially unaffected in both POM/PU/LS (DM) and POM/PU/LS (MB) systems.

(iii) δ-mode, attributed to defect dipoles in the crystalline phase of POM, is significantly influenced by the preparation technique.

(iv) α-mode of POM shifts to higher frequencies in POM/PU/LS (MB) systems with respect to their DM produced counterparts.

(v) In both cases, the incorporation of LS results in the separation of γ- and δ-modes of POM, either as two distinct relaxation peaks (DM system) or as a broad peak (MB system) which is deconvoluted in the two separate contributions.

This research did not receive any specific grant from funding agencies in the public, commercial, or not-for-profit sectors.

References

[1] D.D. Chung, Composite materials: functional materials for modern technologies, Springer-Verlag, London, 2003.

[2] S. Anandhan, S. Bandyopadhyay, Polymer Nanocomposites: From Synthesis to Applications, in: J. Cuppoletti, (Ed.), Nanocomposites and Polymers with Analytical Methods, InTech, 2011.

[3] G.C. Psarras, Conductivity and dielectric characterization of polymer nanocomposites, in S.C. Tjong, Y.M. Mai (Eds), Polymer nanocomposites: physical properties and applications, Woodhead Publishing Limited, Cambridge, 2010. pp 31-69.

[4] W.H. Zhong, B. Li, Polymer Nanocomposites for Dielectrics, Pan Stanford Publishing Pte. Ltd. Singapore, 2017.

[5] C.J. Plummer, P. Scaramuzzino, H.H. Kausch, J.M. Philippoz, High temperature slow crack growth in polyoxymethylene. Polym. Eng. Sci. 40 (2000) 1306-1317.

[6] T. Sukhanova, V. Bershtein, M. Keating, G. Matveeva, M. Vylegzhanina, V. Egorov, N. Peschanskaya, P. Yakushev, E. Flexman, S. Greulich, B. Sauer, K. Schodt, Morphology and properties of poly (oxymethylene) engineering plastics, Macromol. Sy. 214 (2004) 135-146.

[7] S. Siengchin, J. Karger-Kocsis, G.C. Psarras, R. Thomann, Polyoxymethylene/polyurethane/alumina ternary composites: Structure, mechanical, thermal and dielectric properties, J. Appl. Polym. Sci. 110 (2008) 1613-1623.

[8] L. Sigrid, P.M. Visakh, Polyoxymethylene: State of Art, New Challenges and Opportunities, in L. Sigrid, P.M. Visakh, S. Chandran (Eds.), Polyoxymethylene Handbook: Structure, Properties, Applications and Their Nanocomposites, Scrivener Publishing, Massachusetts, 2014 pp. 1-20.

[9] C.J.G. Plummer, P. Menu, N. Cudré-Mauroux, H.-H. Kausch, The effect of crystallization conditions on the properties of polyoxymethylene. J. Appl. Polym. Sci. 55 (1995) 489-500.

[10] W. Xu, M. Ge, P. He, Nonisothermal crystallization kinetics of polyoxymethylene/montmorillonite nanocomposite, J. Appl. Polym. Sci. 82 (2001) 2281-2289.

[11] K. Pielichowski, A. Leszczynska, Structure–property relationships in polyoxymethylene/thermoplastic polyurethane elastomer blends. J Polym Eng 25 (2005) 359-373.

[12] W. Tang, H. Wang, J. Tang, H. Yuan, Polyoxymethylene/thermoplastic polyurethane blends compatibilized with multifunctional chain extender, J Appl Polym Sci 127 (2013) 3033-3039.

[13] M. He, D. Zhang, J. Guo, S. Qin, X. Ming, Mechanical, thermal, and dynamic mechanical properties of long glass fiber-reinforced thermoplastic polyurethane/polyoxymethylene composites, Polym Composite 35 (2014) 2067-2073.

[14] A. Leszczyńska, K. Pielichowski, Nanocomposites of Polyoxymethylene, in L. Sigrid, P.M. Visakh, S. Chandran (Eds.), Polyoxymethylene Handbook: Structure, Properties, Applications and Their Nanocomposites, Scrivener Publishing, Massachusetts, 2014 pp. 331-397.

[15] M. Davies, Dielectric and related molecular processes (Vol. 1), The Chemical Society, London, 1972.

[16] N.G. McCrum, B.E. Read, G. Williams, Anelastic and dielectric effects in polymeric solids, John Wiley & Sons, New York, 1967.

[17] A. Vassilikou-Dova, I.M. Kalogeras, Dielectric analysis (DEA), in J.D. Menczel, R.B. Prime (Eds), Thermal analysis of polymers: Fundamentals and applications, John Wiley, Hoboken, New Jersey,2009, pp. 497-613.

[18] F. Kremer, A. Schönhals, Broadband Dielectric Spectroscopy. Springer, Berlin, 2002.

[19] B.E. Read, G. Williams, The dielectric and dynamic mechanical properties of polyoxymethylene (Delrin), Polymer 2 (1961) 239-255.

[20] C.H. Porter J.H. Lawler, R.H. Boyd, A Dielectric Study of Molecular Relaxation in Polyoxymethylene at High Temperatures, Macromolecules 3 (1970) 308-314.

[21] Y.S. Papir, E. Baer, The internal friction of polyoxymethylene from 4.2° to 300° K, Mater. Sci. and Eng. 8 (1971) 310-322.

[22] R.W. Gray, On the α-relaxation in bulk polyoxymethylene, J. Mater. Sci. 8 (1973) 1673-1689.

[23] R.J.V. Hojfors, E. Baer, P.H. Geil, Dynamic-mechanical study of molecular motions in solid polyoxymethylene copolymers from 4 to 315 K, J. Macromol. Sci. B 13 (1977) 323-348.

[24] J.B. Enns, R. Simha, Transitions in semicrystalline polymers. II. Polyoxymethylene and poly (ethylene oxide), J. Macromol. Sci. B 13 (1977) 25-47.

[25] M.E. Kazen, P.H. Geil, Electron microscopy studies of relaxation behavior of polyoxymethylene), J. Macromol. Sci. B 13 (1977). 381-404.

[26] H.W. Starkweather Jr., Simple and complex relaxations, Macromolecules 14 (1981) 1277-1281.

[27] R.H. Boyd, Relaxation processes in crystalline polymers: molecular interpretation—a review, Polymer 26 (1985) 1123-1133.

[28] B B. Sauer, P. Avakian, E.A. Flexman, M. Keating, B.S. Hsiao, R.K. Verma, AC dielectric and TSC studies of constrained amorphous motions in flexible polymers including poly (oxymethylene) and miscible blends, J. Polym. Sci. Pol. Phys. 35 (1997) 2121-2132.

[29] D.A. Wasylyshyn, Effects of moisture on the dielectric properties of polyoxymethylene (POM). IEEE T. Dielect. El. In. 12 (2005) 183-193.

[30] V.A. Bershteina, L.M. Egorovaa, V.M. Egorova, N.N. Peschanskayaa, P.N. Yakusheva, M.Y. Keatingb, E.A. Flexmanb, R.J. Kassalb, K.P. Schodtb, Segmental dynamics in poly (oxymethylene) as studied via combined differential scanning calorimetry/creep rate spectroscopy approach, Thermochim. acta, 391 (2002) 227-243.

[31] G. Kumaraswamy, N.S. Surve, R. Mathew, A. Rana, S.K. Jha, N.N. Bulakh, A.A. Nisal, T.G. Ajithkumar, P.R. Rajamohanan, Lamellar melting, not crystal motion, results in softening of polyoxymethylene on heating, Macromolecules, 45 (2012) 5967-5978.

[32] P.K. Karahaliou, A.P. Kerasidou, S.N. Georga, G.C. Psarras, C.A. Krontiras, J. Karger-Kocsis, Dielectric relaxations in polyoxymethylene and in related nanocomposites: Identification and molecular dynamics, Polymer 55 (2014) 6819-6826.

[33] Y. Ishida, M. Matsuo, H. Ito, M. Yoshino, F. Irie, M. Takayanagi, Dielectric behavior and visco-elastic behavior of polyoxymethylene (Delrin), Colloid Polym. Sci. 174 (1961) 162-163.

[34] K. Arisawa, K. Tsuge, Y. Wada, Dielectric Relaxations in Polyoxymethylene and Polyethylene Oxide, JPN J Appl. Phys. 4 (1965) 138.

[35] J.M. Machado, R.N. French, Miscible polyacetal-poly (vinyl phenol) blends: 2. Thermomechanical properties and morphology, Polymer 33 (1992) 760-766.

[36] G.C Psarras, S. Siengchin, P.K Karahaliou, S.N Georga, C.A Krontiras, J. Karger-Kocsis. Dielectric relaxation phenomena and dynamics in polyoxymethylene/polyurethane/alumina hybrid nanocomposites, Polym. Int. 60 (2011) 1715-1721.

[37] K.G. Gatos, J.G. Martínez Alcázar, G.C. Psarras, R. Thomann, J. Karger-Kocsis, Polyurethane latex/water dispersible boehmite alumina nanocomposites: Thermal, mechanical and dielectrical properties, Compos. Sci. Technol. 67 (2007) 157-167.

[38] G.C. Psarras, K.G. Gatos, P.K. Karahaliou, S.N. Georga, C.A. Krontiras, J. Karger-Kocsis, Relaxation phenomena in rubber/layered silicate nanocomposites. Express Polym. Lett. 1 (2007) 837-845.

[39] A. Kalini, K.G. Gatos, P.K. Karahaliou, S.N. Georga, C.A. Krontiras, G.C. Psarras, Probing the dielectric response of polyurethane/alumina nanocomposites, J. Polym. Sci. Pol. Phys. 48 (2010) 2346-2354.

[40] K.W. Wagner, Erklärung der dielektrischen nachwirkungsvorgänge auf grund maxwellscher vorstellungen, Electr. Eng. 2 (1914) 371-387.

[41] R.W. Sillars, The properties of a dielectric containing semiconducting particles of various shapes, Instit. Electr. Eng. 12 (1937) 139-155.

[42] S. Havriliak, S. Negami, A complex plane analysis of α-dispersions in some polymer systems, J. Polym. Sci. Pol. Sym.14 (1966) 99-117.

[43] S. Havriliak, S.A. Negami, Complex plane representation of dielectric and mechanical relaxation processes in some polymers, Polymer 8 (1967) 161-210.

[44] G.C. Psarras, A. Soto Beobide, G.A. Voyiatzis, P.K. Karahaliou, S.N. Georga, C.A. Krontiras, J. Sotiropoulos, Dielectric and Conductivity Processes in Poly (ethylene terephthalate) and Poly (ethylene naphthalate) Homopolymers and Copolymers, J. Polym. Sci. Pol. Phys. 44 (2006) 3078-3092.

[45] G.N. Tomara, A.P. Kerasidou, A.C. Patsidis, P.K. Karahaliou, G.C. Psarras, S.N. Georga, C.A. Krontiras, Dielectric response and energy storage efficiency of low content TiO_2-polymer matrix nanocomposites, Compos. Part A-Appl. S. 71 (2015) 204-211.

[46] S. Charlon, L. Delbreilh, E. Dargent, N. Follain, J. Soulestin, S. Marais, Influence of crystallinity on the dielectric relaxations of poly (butylene succinate) and poly [(butylene succinate)-co-(butylene adipate)], Eur. Polym. J. 84 (2016) 366-376.

[47] S. Siengchin, Dynamic mechanic and creep behaviors of polyoxymethylene/boehmite alumina nanocomposites produced by water-mediated compounding: Effect of particle size, J. Thermoplast. Compos. 26 (2013) 863-877.

Figure captions

Fig.1. SEM images of POM/PU/LS nanocomposites produced via DM compounding (a) and MB technique (b). Note: holes and spherical domains represent PU and arrows indicate for LS.

Fig.2. TEM images of POM/PU/LS composites produced via the MB technique

Fig.3. Frequency and temperature variation of the imaginary part of electric modulus (M") for the POM/PU/LS nanocomposite produced via (a) DM compounding and (b) MB technique. *In the plots MWS and CT stand for Maxwell-Wagner-Sillars effect and conductivity term respectively.*

Fig.4. Loss factor versus frequency for the (a) POM/PU/LS (DM) and (b) POM/PU/LS (MB) system in the low temperature region.

Fig.5. Deconvolution of the dielectric loss spectra (ε") into the γ-mode and δ-mode of POM and γ-mode of PU in the frequency domain for (a) POM/PU/LS (DM) and (b) POM/PU/LS (MB) system, at -90°C.

Fig.6. Comparative graph of the fitted results of dielectric loss ε" versus frequency for the POM/PU/LS (DM) and POM/PU/LS (MB) systems, at -80°C.

Fig.7. Loss factor versus frequency for the (a) POM/PU/LS (DM) and (b) the POM/PU/LS (MB) systems in the high temperature region. *In the plots MWS and CT stand for Maxwell-Wagner-Sillars effect and conductivity term respectively.*

Fig.8. Deconvolution of the dielectric loss ε" versus frequency into the α-modes of PU and POM in the frequency domain for the (a) POM/PU/LS (DM) and (b) POM/PU/LS (MB) systems at 60°C.

Fig.9. Comparative graph of the fitting results in dielectric modulus M" representation for the POM/PU/LS (DM) and POM/PU/LS (MB) systems at 90°C. Inset: Deconvolution of the dielectric loss ε" versus frequency into the α-modes of PU and POM and the conductivity term (CT) in the frequency domain for the POM/PU/LS (DM) system at the same temperature. *In the plots MWS and CT stand for Maxwell-Wagner-Sillars effect and conductivity term respectively.*

Fig.10. Relaxation time versus inverse temperature for the (a) low and (b) high temperature modes of POM/PU/LS (DM) and POM/PU/LS (MB) systems.

Tables

Table 1. Activation energies and VTF parameters as calculated from the fitting results, for all compared systems.

sample	**α mode POM**	**α mode PU**		**γ mode POM**	**δ mode POM**	**γ mode PU**
	E_A (eV)	B (K)	T_o (K)	E_A (eV)	E_A (eV)	E_A (eV)
POM/PU/LS (DM)	0.43	1395	165	0.85	0.68	0.52
POM/PU/LS (MB)	0.33	994	185	0.69	0.72	0.75
pure PU						0.45